Anomalous behaviour in the phase transition and crystal structure of urea adducts with *n*-eicosane

1996 J. Phys.: Condens. Matter 8 2105

(http://iopscience.iop.org/0953-8984/8/13/003)

J. Phys.: Condens. Matter **8** (1996) 2105–2118. Printed in the UK

Anomalous behaviour in the phase transition and crystal structure of urea adducts with *n*-eicosane

Koji Fukao

Department of Fundamental Sciences, Faculty of Integrated Human Studies, Kyoto University, Kyoto 606-01, Japan

Received 27 November 1995, in final form 2 February 1996

Abstract. X-ray diffraction measurements are made for urea adducts with *n*-eicosane to investigate the arrangement of *n*-eicosane molecules in the channels formed by urea molecules. Extra Bragg reflections have been found on the layers with the q_z-coordinate corresponding to twice the chain length of the *n*-eicosane molecule in both the low- and high-temperature phases. This kind of Bragg reflection has not been observed for other *n*-alkanes in urea adducts. On the basis of the intensity distribution of the extra Bragg reflections, it is found that the *n*-eicosane molecules are arranged in such a way that the orientations of zigzag planes of longitudinally neighbouring molecules are anti-parallel to each other.

1. Introduction

N-alkane molecules can be included regularly and closely in the hexagonal channel of urea molecules to form an inclusion compound called a urea adduct [1]. It is well known that the urea inclusion compound with *n*-alkanes exhibits a phase transition from the hexagonal high-temperature phase to the orthorhombic low-temperature phase as the temperature is lowered from room temperature to the transition temperature T_t [2]. Many experiments such as Raman [3–5], x-ray scattering [6, 7, 8], and neutron scattering [9, 10] studies have elucidated the nature of the phase transition; in the hexagonal phase the alkane molecules included are subject to various kinds of disorder such as rotational and oscillational disorder around the chain axis, translational disorder along the chain axis and conformational disorder within a chain [11–13].

Because the origin of this phase transition is related to the onset of disorder of included *n*-alkanes, we can expect similarity between the phase transition of urea adducts and the rotational phase transition of pure *n*-alkane crystals. In fact, the dependence of T_t on the number of carbon atoms n is very similar to that of pure *n*-alkane crystals; T_t increases monotonically with increasing n, although there is a constant shift to lower temperature and a small deviation from the expected smooth curve, compared with the case for T_t of pure *n*-alkanes. So far, the slight deviation from the smooth curve has been thought to be due to the incommensurate relation between the chain length of *n*-alkane molecules and the lattice constant along the *c*-axis of the urea host lattice. The constant shift comes from the weaker interaction between alkane molecules neighbouring laterally because of the existence of the urea host lattice between them. If the aforementioned deviation is negligible, it can be thought that the mechanism of the phase transition of urea adducts with *n*-alkanes is similar to that of the rotational phase transition of pure *n*-alkane crystals. In a previous paper, it

0953-8984/96/132105+14$19.50

proved that the properties of the phase transitions of both urea adducts with *n*-alkanes and pure *n*-alkanes could successfully be accounted for with a simple model [11]. Assuming that a conformational disorder such as a twist or soliton is created at the phase transition temperature, the dependence of T_t on n and on pressure, and the change in the enthalpy at T_t could well be reproduced in both the cases.

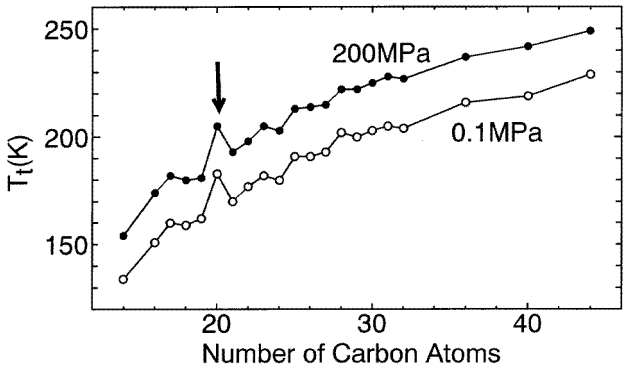

Figure 1. The dependence of the transition temperature T_t on the number of carbon atoms n at 0.1 MPa and 200 MPa for urea adducts with *n*-alkanes ($n = 14$–44). The values of T_t are obtained via differential thermal analysis for high pressures [14]. The arrow shows the anomaly at $n = 20$.

Despite the success in finding the common feature between the mechanism of the phase transition of urea adducts with *n*-alkanes and that of pure *n*-alkanes, it is known that T_t of *n*-eicosane in urea adducts is exceptionally higher than the expected value from T_ts around $n = 20$ [2, 14]. Figure 1 shows that T_t of *n*-eicosane/urea adducts is higher by about 20 K than the expected value, although the small deviation mentioned above is at most 5 K from the smooth curve. Anomalous behaviours of *n*-eicosane/urea adducts have been observed not only in the *n*-dependence of T_t but also in the chain-length dependence of the energy barrier E^* of rotational motion of *n*-alkane molecules around the chain axis. The dependence of E^* on the chain length has been estimated by Kobayashi *et al* from the observed temperature dependences of a band width of Raman scattering [5].

These experimental results strongly suggest the existence of a structural anomaly in the arrangement of *n*-eicosane molecules in urea adducts. In this paper x-ray diffraction measurements are made to investigate the arrangement of *n*-eicosane molecules in urea adducts, to compare the structure of *n*-eicosane in urea adducts with that of other *n*-alkanes, and to discuss the relationship between the arrangement of *n*-alkanes and T_t.

2. Experimental details

Samples used in this work were single crystals of urea adducts with *n*-tridecane (*n*-$C_{13}H_{28}$, C13), and *n*-eicosane (*n*-$C_{20}H_{42}$, C20). Reagents of urea and *n*-alkanes were purchased from Nakarai Chemical Co. Ltd. No further purification was undertaken. The preparation method of the single crystals was the same as described previously [8]. The transition temperature T_t of the crystals used in this study was 183 K for $n = 20$. Single crystals of urea adducts with *n*-alkanes were placed in a flow of nitrogen gas whose temperature was controlled by using a Nitrogen Cryostat (FR558NH, Enraf–Nonius Co.) in the range 136 K–329 K. Monochromatized Cu Kα radiation was used as an incident beam, and intensities of the

Bragg reflections were measured using a Weissenberg counter diffractometer (STOE Co., Darmstadt, Germany). X-ray oscillation photographs were also taken at various temperatures using flat films. Observed intensities were corrected for the polarization factor and the relative intensities were independent of whether integrated intensity or peak intensity was used within experimental accuracy.

3. Results

The diffraction patterns of urea adducts with *n*-eicosane were observed from x-ray oscillation photographs around the c^*-axis (the chain axis). Segments of the x-ray photographs at room temperature, 192 K and 136 K are compared in figure 2, (a)–(c). A schematic picture of the segment at a lower temperature is also given, in figure 2(d). Several kinds of contribution can be seen in these photographs. In order to clarify the overall diffraction patterns schematic drawings of the intensity distributions in the reciprocal space of the scattered x-rays of *n*-$C_{20}H_{42}$/urea adducts are given in figure 3(a) for room temperature, in figure 3(b) for a lower temperature that is still above T_t, and in figure 3(c) for below T_t. The distributions were estimated by using the x-ray oscillation photographs and a counter method. It should be noted that the intensity distributions around the meridian ($q_\rho = 0$) in figure 3 were estimated by a counter method, because x-ray photographs taken by oscillation around the c^*-axis in figure 2 can give us no information around the meridian.

In figure 2(d) and figure 3 the contributions from the urea host lattice are *not* described, although the x-ray diffraction patterns of single crystals of urea adducts with *n*-alkanes have both many strong Bragg reflections of the urea host lattice and some Bragg reflections of the included *n*-alkane molecules as shown in figure 2, (a)–(c). The positions of the former do not change with the molecular length of *n*-alkanes, while the latter exists on reciprocal-lattice planes whose location along the c^*-axis varies proportionally to the reciprocal of the molecular length. The strong Bragg reflections which appear in figure 2, (a)–(c), but disappear in the schematic drawing of figure 2(d) are the contributions from the urea host lattice. In figure 3 there would be Bragg reflections from the urea host lattice on the layer with $q_z = 0.57$, 1.14, 1.71, 2.28, and 2.85 Å^{-1}, if the contributions from urea molecules were taken into consideration. In figure 3 we can find at least four different types of scattering from *n-eicosane,* not from the urea host lattice, included in the channel formed by urea molecules at temperatures from 136 K to room temperature as detailed below.

(1) Streak-like diffuse scattering whose width along the c^*-axis is as sharp as that of Bragg reflections (s diffuse scattering). The q_z-coordinates of the s diffuse scattering are related to the chain length of *n*-eicosane around the equator, while they are related to twice the chain length around the first layer of the subcell, i.e., the unit cell of the structure of C_2H_4 repeating units.

(2) Broad diffuse scattering around the first layer of the subcell (d diffuse scattering).

(3) Bragg reflections on the layer whose q_z-coordinate corresponds to the chain length of *n*-eicosane (open circles in figure 3).

(4) Bragg reflections whose q_z-coordinates correspond to twice the chain length of *n*-eicosane molecules and which do not belong to type (3) (full circles in figure 3). Around the equator the Bragg reflections of this type exist between the layers of the streak-like diffuse scattering, while around the first layer of the subcell they exist on the streak-like diffuse scattering.

The nature of the diffuse scattering of types (1) and (2) has been discussed in detail in our previous papers [8]. The Bragg reflections of type (3) are associated with the fact

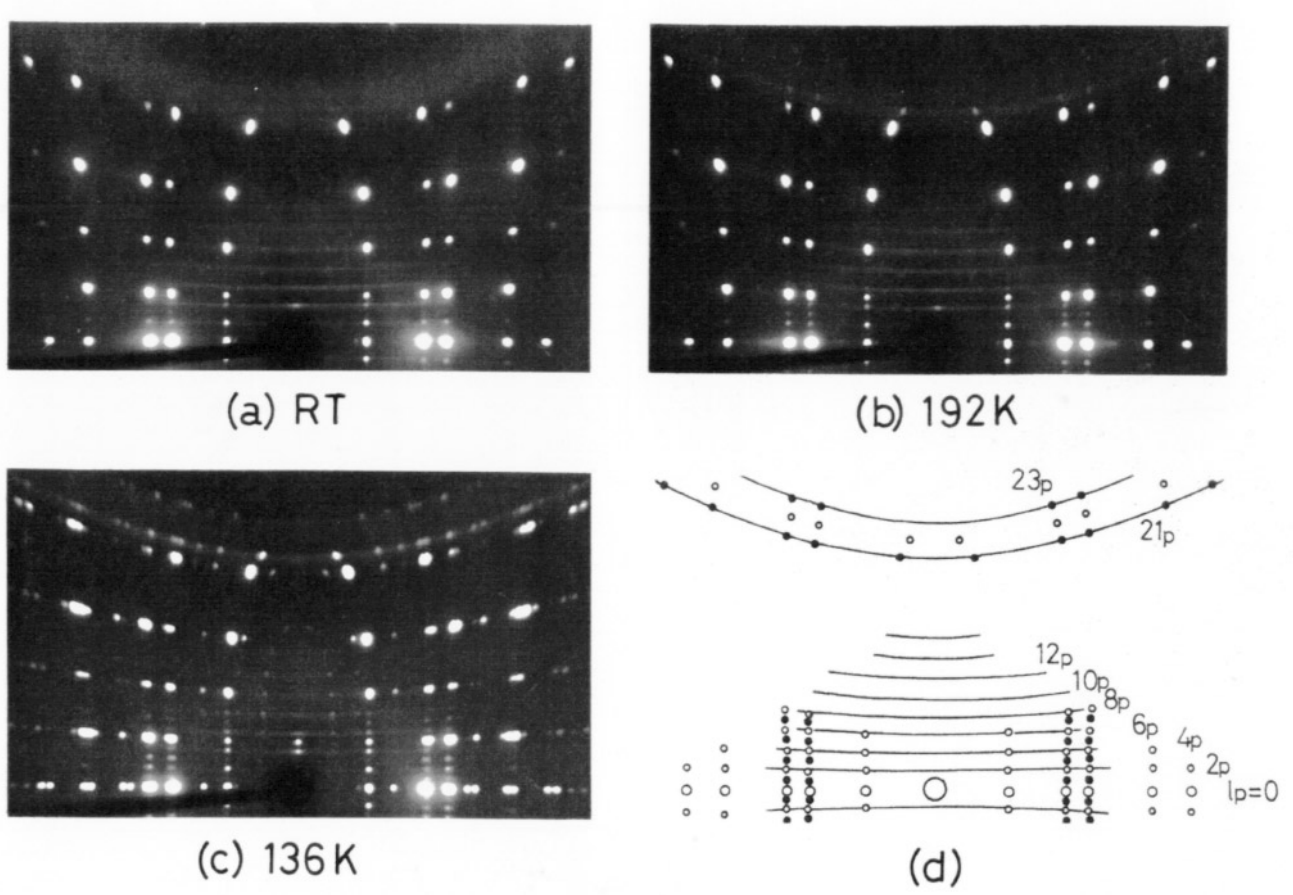

Figure 2. X-ray oscillation photographs around the chain axis of single crystals of urea adducts with n-$C_{20}H_{42}$ at various temperatures. They were taken on flat films. (a) Room temperature. (b) 192 K. (c) 136 K. (d) A schematic drawing of the x-ray scattering from n-eicosane molecules. The contributions from the urea host lattice, which appear in (a)–(c), are not described in (d). The numbers given in (d) are the Miller indices l_p of the layers perpendicular to the c^*-axis (q_z-axis)

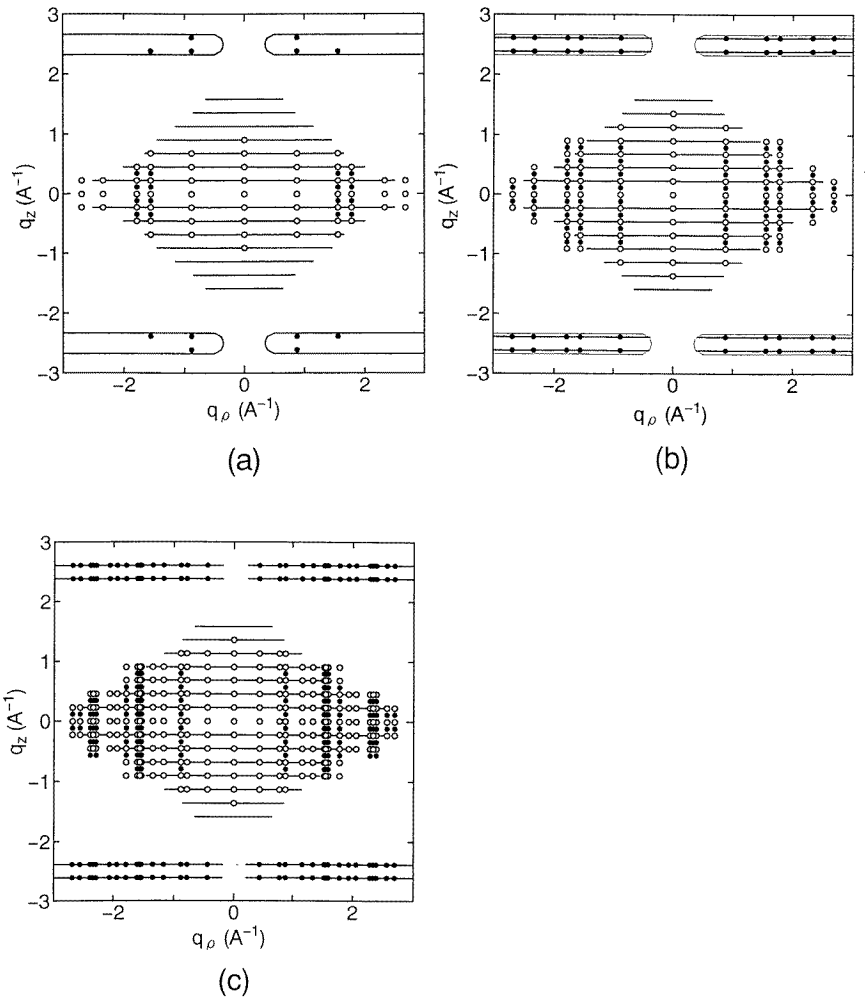

Figure 3. Schematic drawings of the distributions in reciprocal space of the x-ray scattering intensity obtained from oscillation photographs around the chain axis and using a counter method. (a) Room temperature. (b) Lower temperature—but still above T_t. (c) Below T_t. Here a cylindrical coordinate (q_ρ, ϕ, q_z) is used for a scattering vector $\boldsymbol{q}$. The contributions from all azimuthal angles ϕ are superimposed. The Bragg reflections from the urea host lattice are not described in these figures. The open circles (○), full circles (●) and straight lines (−) stand for the contributions of types (3), (4) and (1), defined in the text, respectively. In the rounded area around $q_z \sim \pm 2.5$ Å^{-1} there is d diffuse scattering, i.e., the contributions of type (2).

that n-alkane molecules in the planar zigzag conformation are arranged regularly in the three-dimensional space. The contributions (1)–(3) are observed commonly in urea adducts with n-alkanes, except the q_z-coordinates of the s diffuse scattering around the first-layer line of the subcell [7, 15]. In addition to the above three contributions, the Bragg reflections of type (4) are observed in the case of n-eicosane in the urea adducts. The full circles in figure 2(d) and figure 3 stand for this type of Bragg reflection. As the temperature decreases, the intensities of the Bragg reflections increase for both types (3) and (4). The increasing

rate of the intensities of type (4) is larger than that of type (3).

When the temperature decreases through T_t down to 136 K, the phase transition occurs and the crystal symmetry changes from hexagonal to orthorhombic. The reflections with $h + k =$ odd integer disappear due to the extinction rule in the high-temperature hexagonal phase. When the symmetry changes from hexagonal to orthorhombic, the extinguished reflections appear in the low-temperature orthorhombic phase [2]. The Bragg reflections of this type can easily be recognized by comparing figure 3(b) with figure 3(c). Here it should be emphasized that the Bragg reflections of type (4), which correspond to doubling of the lattice constant along the c-axis, exist both in the high-temperature hexagonal phase and in the low-temperature orthorhombic one. The existence of the doubling of the c-axis has not so far been reported for other urea adducts.

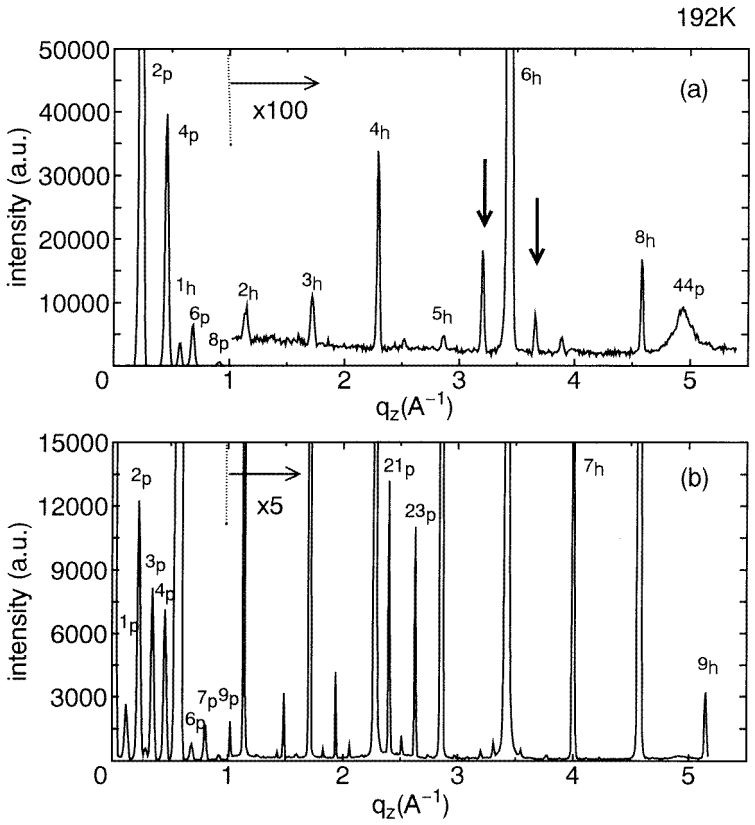

Figure 4. The dependence of the scattering intensity at 192 K in the urea adducts with n-eicosane on q_z (a) along the meridian and (b) along the $[13\zeta]^*$ axis. The intensity of $q_z > 1$ Å^{-1} is multiplied by a factor of (a) 100 and (b) 5. The numbers with suffices p and h are Miller indices defined by equation (1).

Figure 4 shows the x-ray scattering intensity along the meridian and the $[13\zeta]^*$ axis for urea adducts with n-$C_{20}H_{42}$ at 192 K. In figure 4 we can find two types of Bragg reflection: the Bragg reflection of the urea host lattice and the one of the regular arrangement of n-eicosane included in the urea adducts. The numbers with suffices p and h in figure 4 stand

for the Miller index using the relation

$$q_z = \frac{2\pi l_p}{c_p} = \frac{2\pi l_h}{c_h} \tag{1}$$

where q_z is the c^*-component of the scattering vector, c_h is the period along the c-axis of the urea host lattice ($c_h = 11.005$ Å at room temperature for n-$C_{16}H_{34}$ [1]), and c_p is the period of the arrangement along the c-axis of n-alkanes included in urea adducts. In the case of C20, $c_h = 11.005$ Å and $c_p = 2L_p$, where L_p is the molecular length along the chain axis of n-eicosane in the planar zigzag conformation ($L_p = 27.68$ Å for C20) [16].

Figure 4(b) shows that the intensity of the Bragg reflections with even l_p is stronger than that of those with odd l_p near the equator along the $[13\zeta]^*$ axis, while only the Bragg reflections with odd l_p, $l_p = 21_p$ and 23_p, are observed near $q_z \sim 2.5$ Å^{-1} which corresponds to the first layer of the subcell of C_2H_4 repeating units. In contrast to the results of figure 4(b), there are only Bragg reflections with even l_p along the meridian as shown in figure 4(a); no extra Bragg reflections due to the doubling of the c-axis related to the arrangement of n-eicosane are observed on the meridian.

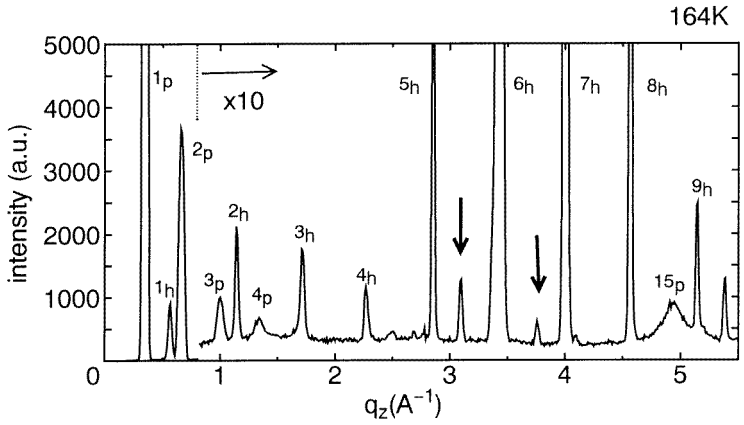

Figure 5. The dependence of the scattering intensity along the meridian at 164 K in the urea adducts with n-tridecane. The reflections indicated by arrows are satellite reflections of 006_h. In this case the Miller index l_p is defined by $q_z = 2\pi l_p/L_p$, where L_p is the molecular length of C13 ($L_p = 18.86$ Å [16]).

Another type of Bragg reflection, of which examples are indicated by arrows in figure 4(a), also exists along the meridian. The Bragg reflections can be attributed to the modulation of the urea host lattice along the c-axis with a period of L_p, although the positions of the two reflections are equal to those of the 0028_p and 0032_p reflections, respectively. Hence, the two reflections are satellite reflections of the 006_h reflection. This does not arise from a special situation for C20, but is a common feature in the urea adducts with n-alkanes. Figure 5 shows the existence of the satellite reflections on the meridian in urea adducts with n-tridecane (C13), in which case there is no commensurate relation between c_h and c_p (or L_p). In the case of C20 the satellite reflection may exist not only for the $hk6_h$ reflection but also around strong Bragg reflections of the urea host lattice. Some weak reflections at $q_z = 1.5$–2.0, 3.0–4.0 Å^{-1} in figure 4(b) may be such satellite reflections. However, we believe that other reflections with suffix p arise mainly from the regular arrangement of n-eicosane molecules because the structure factor of n-alkane of

the planar zigzag conformation has appreciable value only near the equator and around the layer line of the subcell ($q_z \sim 2.5$ Å^{-1}, 5.0 Å^{-1}, ...).

The existence of the extra reflections, the Bragg reflections with odd l_p, in urea adducts with n-eicosane suggests a superlattice structure whose period along the c-axis is twice the chain length of n-eicosane molecules included in the urea host lattice. The fact that the length along the chain axis of two n-eicosane molecules neighbouring longitudinally in the hexagonal channel is five times as long as c_h may cause the superlattice structure. The absence of the extra Bragg reflections on the meridian suggests that the one-dimensional structure reflected onto the c-axis has no superlattice structure. Therefore, the superlattice structure is due only to the modulation of the crystal structure within a plane normal to the chain axis.

4. The model for the scattering intensity

In this section, a model is introduced for the x-ray scattering intensity in order to discuss the superlattice structure observed in urea adducts with n-eicosane. Since n-alkane molecules in urea adducts have a planar zigzag conformation, we can regard an n-alkane molecule as a helical polymer with a finite molecular length and in 2/1 helical conformation. The diffraction theory of helical polymers has already been developed by many researchers and the structure factors of helical polymers can well be described by cylindrical coordinates of positional vectors of atoms and a scattering vector, and by Bessel functions [17].

In the case of n-eicosane in urea adducts we should regard two n-alkane molecules neighbouring longitudinally in the hexagonal channel as a structural unit to account for the existence of the superlattice reflections. The two molecules are distinguished by the symbols (+) and (−). If we assume that the positional vectors $\boldsymbol{r}_j^{(\pm)}$ of the jth carbon atom of the (±) n-alkane molecule are expressed by

$$\boldsymbol{r}_j^{(\pm)} = (\rho_{Cj}, \varphi_j^{(\pm)}, z_j^{(\pm)})$$

in terms of cylindrical coordinates, respectively, the structure factor of the two molecules can be defined by

$$F_{2m}(\boldsymbol{q}) = \sum_{j=1}^{n} (f_C(\boldsymbol{q}) \mathrm{e}^{\mathrm{i}\boldsymbol{q}\cdot\boldsymbol{r}_j^{(+)}} + f_C(\boldsymbol{q}) \mathrm{e}^{\mathrm{i}\boldsymbol{q}\cdot\boldsymbol{r}_j^{(-)}})$$

where $\boldsymbol{q}$ is a scattering vector, (q_ρ, ϕ, q_z) is the component of the cylindrical coordinate of $\boldsymbol{q}$, f_C is the atomic scattering factor of a carbon atom, and n is the number of carbon atoms of a molecule. Using an expansion formula with Bessel functions J_k

$$\mathrm{e}^{\mathrm{i}z\cos\theta} = \sum_{k=-\infty}^{\infty} \mathrm{i}^k J_k(z) \mathrm{e}^{\mathrm{i}k\theta}$$

the structure factor F_{2m} can be written as

$$F_{2m}(\boldsymbol{q}) = \sum_{k=-\infty}^{\infty} f_C(\boldsymbol{q}) \mathrm{i}^k J_k(q_\rho \rho_C) \mathrm{e}^{-\mathrm{i}k\phi} \sum_{j=1}^{n} \mathrm{e}^{\mathrm{i}(k\varphi_j^{(-)} + q_z z_j^{(-)})} + \sum_{k=-\infty}^{\infty} f_C(\boldsymbol{q}) \mathrm{i}^k J_k(q_\rho \rho_C) \mathrm{e}^{-\mathrm{i}k\phi} \sum_{j=1}^{n} \mathrm{e}^{\mathrm{i}(k\varphi_j^{(+)} + q_z z_j^{(+)})} \quad (2)$$

where J_k is the kth-order Bessel function and it is assumed that $\rho_{Cj} = \rho_C$ (independent of j) [8]. Although contributions from hydrogen atoms attached to the carbon atoms are omitted in the above expression, the contributions have been taken into account when

calculating intensities of Bragg reflections. Furthermore, it is assumed that n-alkane molecules have planar zigzag conformation and the coordinates of the above n-alkane molecules satisfy the relations:

$$z_j^{(+)} = z_j^{(-)} + L_p$$
$$\varphi_j^{(+)} = \varphi_j^{(-)} + \tilde{\varphi}_{\pm}.$$

This means that n-alkane molecules are aligned exactly at an interval of the chain length along the c-axis in the hexagonal channel, but that the orientations of the zigzag planes of the two molecules neighbouring longitudinally are different from each other by $\tilde{\varphi}_{\pm}$ around the chain axis. The displacements of the centre of mass of n-alkanes perpendicular to the chain axis in a structural unit are neglected because of geometrical restrictions. Then we obtain

$$F_{2m}(\boldsymbol{q}) = \sum_{k=-\infty}^{\infty} f_C(\boldsymbol{q}) \mathrm{i}^k \mathrm{e}^{-\mathrm{i}k\phi} J_k(q_\rho \rho_C) \xi(k, l_p) \eta(k, l_p) \tag{3}$$

where

$$\xi(k, l_p) = 1 + \mathrm{e}^{\mathrm{i}(k\tilde{\varphi}_{\pm} + q_z L_p)} \qquad \eta(k, l_p) = \sum_{j=1}^{n} \mathrm{e}^{\mathrm{i}(k\varphi_j^{(-)} + q_z z_j^{(-)})}.$$

In this case, the coordinates of the jth carbon atom of a n-alkane molecule are given by

$$\rho_{Cj} = \rho_C \qquad \varphi_j^{(-)} = \pi j \qquad z_j^{(-)} = \frac{c_s}{2} j$$

where $\rho_C = 0.43$ Å^{-1} and c_s (= 2.54 Å) is the lattice constant along the c-axis which corresponds to the C_2H_4 repeating unit, namely, the subcell structure. For C20, the lattice constant along the c-axis of included n-alkane molecules is twice L_p ($c_p = 2L_p$). Since the lengths of c_p, c_h, and c_s satisfy the relation $c_p \simeq 5c_h \simeq 22c_s$, we obtain the equations

$$l_p \simeq 5l_h \simeq 22l_s \tag{4}$$

where l_p, l_h, and l_s are Miller indices with respect to c_p, c_h, and c_s, respectively. Hence, the factor $\eta(k, l_p)$ is expressed as

$$\eta(k, l_p) = \sin\frac{\pi n}{2}\left(k + l_p\frac{c_s}{c_p}\right) \Big/ \sin\frac{\pi}{2}\left(k + l_p\frac{c_s}{c_p}\right) = \sin\frac{\pi n}{2}(k + l_s) \Big/ \sin\frac{\pi}{2}(k + l_s) \tag{5}$$

where the phase factor is omitted because it is not important for calculating intensities of Bragg reflections. The factor $\eta(k, l_p)$ is the *Laue interference function* of a single alkane molecule. Hence, we find that due to this factor the Bessel functions J_{2k} have more dominant contributions to the intensities of Bragg reflections near the equator than do the functions J_{2k-1}, while around the first layer line of the subcell ($l_s \simeq 1$) it is the Bessel functions J_{2k-1} that have more dominant contributions to the intensities of Bragg reflections.

The structure factor given by equation (3) consists of all of the contributions from the Bessel functions for different values of k. The factors $\eta(k, l_p)$ and $\xi(k, l_p)$ determine which order of Bessel functions have dominant contributions to the intensity of the Bragg reflections. In this model we assume that $\tilde{\varphi}_{\pm} = \pi$. This means that the orientations of the zigzag planes of the two neighbouring molecules in the channel are anti-parallel to each other. The factor $\xi(k, l_p)$ is then expressed as

$$\xi(k, l_p) = \begin{cases} 2 & k + l_p = \text{even integer} \\ 0 & k + l_p = \text{odd integer.} \end{cases} \tag{6}$$

This relation leads to a selection rule of the order of Bessel functions for the Miller index l_p. For a series of Bragg reflections with l_p = even integer (odd integer), the Bessel functions J_{2k} (J_{2k-1}) are dominant as regards contributions to the intensity of the Bragg reflections. Taking account of the factors $\eta(k, l_p)$ and $\xi(k, l_p)$ we can expect from the model that the intensity of Bragg reflections with l_p = even integer will be stronger near the equator than that with odd l_p, while the intensity of Bragg reflections with odd l_p will be stronger around the first layer line of the subcell. These results agree well with the observed ones in figures 2 and 4, and hence the present model is valid for reproducing the intensities of Bragg reflections from *n*-eicosane in the urea adducts.

In order to discuss the temperature dependence of the scattering intensity, two types of displacement, translational displacement along the chain axis and rotational displacement around the chain axis, are introduced in a similar way to that described in the previous paper [8]:

$$z_j^{(-)} \to z_j^{(-)} + u_z^{(-)} \qquad z_j^{(+)} \to z_j^{(+)} + u_z^{(+)}$$
$$\varphi_j^{(-)} \to \varphi_j^{(-)} + \varphi_0 + \Delta\tilde{\varphi}^{(-)} \qquad \varphi_j^{(+)} \to \varphi_j^{(+)} + \varphi_0 + \Delta\tilde{\varphi}^{(+)}$$

where we assume for simplicity that *n*-alkane molecules have no internal degree of freedom and all structural units within a crystallite have a favoured orientation φ_0 around the chain axis. Furthermore, we assume that the displacements $u_z^{(+)}$, $u_z^{(-)}$, $\Delta\tilde{\varphi}^{(+)}$ and $\Delta\tilde{\varphi}^{(-)}$ obey a Gaussian distribution around zero, have no correlation among them and $\langle u_z^{(+)2}\rangle = \langle u_z^{(-)2}\rangle \equiv \langle u_z^2\rangle$, $\langle \Delta\tilde{\varphi}^{(+)2}\rangle = \langle \Delta\tilde{\varphi}^{(-)2}\rangle \equiv \langle \Delta\tilde{\varphi}^2\rangle$. The symbol $\langle\cdots\rangle$ stands for the average over all unit cells. Then, after averaging φ_0 throughout all crystallites, we obtain the intensity formula as follows:

$$\begin{aligned} I(\boldsymbol{q}) &= |\langle F_{2m}(\boldsymbol{q})\rangle|^2 \left|\sum_{\boldsymbol{r}} \mathrm{e}^{\mathrm{i}\boldsymbol{q}\cdot\boldsymbol{r}}\right|^2 \\ &= \sum_k |f_C(\boldsymbol{q})|^2 J_k^2(q_\rho\rho_C)\mathrm{e}^{-k^2\langle\Delta\tilde{\varphi}^2\rangle}\mathrm{e}^{-q_z^2\langle u_z^2\rangle}|\xi(k,l_p)|^2|\eta(k,l_p)|^2 \sum_{hkl}\delta(\boldsymbol{q}-\boldsymbol{q}_{hkl}) \end{aligned} \tag{7}$$

where $\boldsymbol{q}_{hkl}$ is a reciprocal-lattice vector. From the selection rule imposed by the factor $\xi(k, l_p)$, we obtain for any reciprocal-lattice vector $\boldsymbol{q}$

$$I(\boldsymbol{q} \equiv \boldsymbol{q}_{hkl_p}) \propto \begin{cases} |f_C(\boldsymbol{q})|^2 J_1^2(q_\rho\rho_C)\mathrm{e}^{-\langle\Delta\tilde{\varphi}^2\rangle}\mathrm{e}^{-q_z^2\langle u_z^2\rangle}|\eta(1,l_p)|^2 & l_p = \text{odd} \\ |f_C(\boldsymbol{q})|^2 J_0^2(q_\rho\rho_C)\mathrm{e}^{-q_z^2\langle u_z^2\rangle}|\eta(0,l_p)|^2 & l_p = \text{even} \end{cases} \tag{8}$$

where the higher-order Bessel functions are neglected.

5. Discussion

It can be expected from equation (8) that the q_ρ-dependence of intensities of Bragg reflections will change with the Miller index l_p as follows:

$$I(q_\rho, l_p) \propto \begin{cases} |f_C(\boldsymbol{q})|^2 J_1^2(q_\rho\rho_C) & l_p = \text{odd} \\ |f_C(\boldsymbol{q})|^2 J_0^2(q_\rho\rho_C) & l_p = \text{even.} \end{cases} \tag{9}$$

Figure 6 shows the q_ρ-dependence of the observed intensities of Bragg reflections for various values of q_z or l_p. In figure 6 the intensities of Bragg reflections are normalized by the maximum intensity for l_p = odd integer and by the intensity of the $11l_p$ reflection for l_p = even integer, and all measurements over the temperature range from 192 K to 329 K are

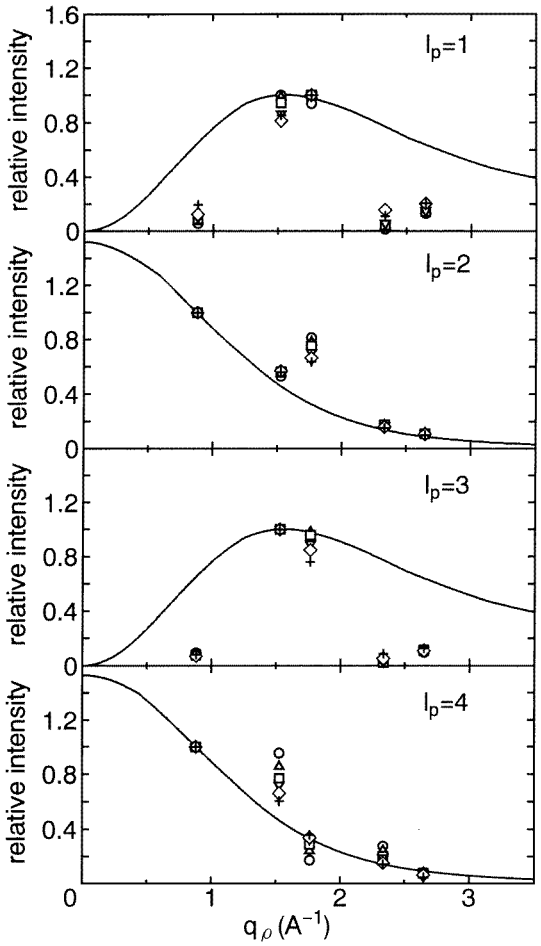

Figure 6. The q_ρ-dependence of relative intensities of Bragg reflections with $l_p = 1$, 2, 3 and 4 in the temperature range from 192 K to 329 K. The solid lines are calculated using equation (9). The intensities with $l_p = 1$ and $l_p = 3$ are normalized by the maximum intensity, while the intensities with $l_p = 2$ and $l_p = 4$ are normalized by the intensity of the $11l_p$ reflections ($q_\rho = 0.881$ Å^{-1}). The symbols show the observed values at various temperatures: ○, 192 K; △, 220 K; □, 248 K; ▽, 276 K; ◇, 303 K; +, 329 K.

plotted. It can easily be found that the intensity of Bragg reflections decreases monotonically with increasing q_ρ for $l_p =$ even integer, while the intensity for $l_p =$ odd integer shows the maximum at around $q_\rho \sim 1.5$ Å^{-1} with increasing q_ρ. The observed q_ρ-dependence can be reproduced by using equation (9) as shown in figure 6 (see the solid lines). (If the effect of the diffuse scattering from the deformation of the urea host lattice is taken into account, the observed intensities of the Bragg reflections around $q_\rho \sim 1.5$ Å^{-1} will be reduced, and then the agreement between the observed and calculated values will be much more strongly enhanced.)

The observed intensities at temperatures above T_t (≡183 K) can be reduced to a master curve for each l_p. This result suggests that the temperature effect can successfully be expressed only in terms of the Debye–Waller factors as shown in equation (8) and there is

no temperature change in the averaged crystal structure.

Equation (8) leads to

$$\log \frac{I(T_0)}{I(T)} = \begin{cases} q_z^2 \Delta\langle u_z^2\rangle + \Delta\langle \Delta\tilde{\varphi}^2\rangle & l_p = \text{odd} \\ q_z^2 \Delta\langle u_z^2\rangle & l_p = \text{even} \end{cases} \tag{10}$$

where

$$\Delta\langle u_z^2\rangle \equiv \langle u_z^2\rangle(T) - \langle u_z^2\rangle(T_0)$$
$$\Delta\langle \Delta\tilde{\varphi}^2\rangle \equiv \langle \Delta\tilde{\varphi}^2\rangle(T) - \langle \Delta\tilde{\varphi}^2\rangle(T_0).$$

$I(T)$ is the intensity at temperature T, and T_0 is the reference temperature. Hence, we can expect that $\log(I(T_0)/I(T))$ should increase linearly with q_z^2 and the slopes of the straight lines will be independent of l_p and that the straight line for l_p = odd should shift in the positive direction along the vertical axis by the value of $\Delta\langle \Delta\tilde{\varphi}^2\rangle$ compared with that for l_p = even.

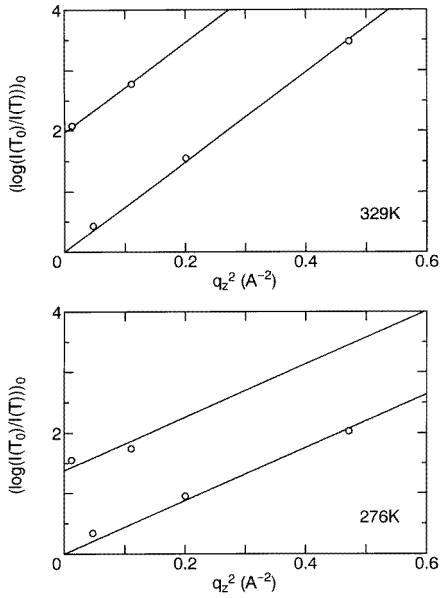

Figure 7. The dependence of $(\log(I(T_0)/I(T)))_0$ on q_z^2 at $T = 276$ K and $T = 326$ K. The reference temperature T_0 is 192 K. The circles stand for the observed values, after correction for the q_ρ-dependence. The solid lines were obtained by using equation (10).

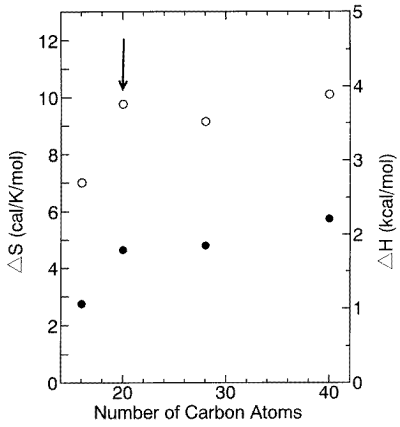

Figure 8. The entropy and enthalpy changes at the phase transition temperature as functions of the number of carbon atoms: ○, ΔS; ●, ΔH. The arrow shows the value at $n = 20$.

The observed values of $\log(I(T_0)/I(T))$ were slightly dependent on q_ρ in the q_ρ-range from 0.881 Å^{-1} to 2.64 Å^{-1}, which suggests that there are contributions from displacements perpendicular to the chain axis in the zigzag plane to the temperature variation in the intensity of Bragg reflections. In order to remove this q_ρ-dependence, we extrapolated the values of $\log(I(T_0)/I(T))$ to the limit $q_\rho^2 \to 0$ for each q_z. The values of $(\log(I(T_0)/I(T)))_0$ thus obtained at $T = 329$ K and 276 K are plotted in figure 7 as functions of q_z^2. The observed values with $l_p = 2, 4$, and 6 fall on a straight line passing through the origin. The values with $l_p = 1$ and 3 also exist on another straight line. The two lines are parallel to each other, and the slopes and y-crossings of the straight lines increase with increasing temperature; the

mean square displacements of u_z and $\Delta\tilde{\varphi}$ increase with temperature. The behaviour agrees well with that expected from equation (10). A least-squares fit of the experimental data to the straight line at various temperatures leads to $\langle u_z^2\rangle$ and $\langle\Delta\tilde{\varphi}^2\rangle$; $\langle u_z^2\rangle = 5.1\times10^{-2}T$ and $\langle\Delta\tilde{\varphi}^2\rangle = 1.2\times10^{-2}T$. These values are greater than those obtained previously for other *n*-alkanes in urea adducts [8]. The quantitative discrepancy may be caused by the non-Gaussian effect of u_z and $\Delta\tilde{\varphi}$ [6, 8], which is neglected in the present model, or by the superposition of strong diffuse scattering existing along the c^*-axis around $q_\rho = 1.3$–2.2 Å^{-1} onto the Bragg reflections. If these two effects can be adequately eliminated, much better quantitative agreement can be obtained.

Within the present model we could reproduce not only the overall properties of the scattering pattern from *n*-eicosane in urea adducts, but also the temperature variation in intensities of the Bragg reflections in the temperature range above T_t. This suggests the validity of the assumption that $\tilde{\varphi}_\pm$ is 180°, which was made in the last section, and hence we can conclude that the orientations of zigzag planes of *n*-eicosane molecules neighbouring longitudinally tend to be anti-parallel. This result may seem surprising because the repulsive interaction between two terminal methyl groups would cause even-numbered *n*-alkane molecules to be parallel to each other [18]. In this case the interaction between the urea host lattice and *n*-eicosane may overcome the repulsive interaction between the methyl groups. Furthermore, the reorientational motion around the chain axis may be large enough to smear out the repulsive interaction.

The present analysis in terms of the model is restricted to measurements above the transition temperature. Below T_t, however, the reorientational motion around the chain axis should be suppressed, and then there may be the possibility that the value of $\tilde{\varphi}_\pm$ has slightly deviated from 180°. Nevertheless, the x-ray photographs shown in figure 2 deny the possibility of parallel orientation in the chain direction below the transition temperature.

In this paper, we were able to elucidate the peculiarity in the arrangements of *n*-eicosanes in urea adducts, compared with that of other *n*-alkanes in urea adducts. Naturally, the peculiarity of the crystal arrangements of *n*-eicosane in urea adducts should be associated with anomalous behaviours in T_t and also in E^*. We show here the relationship between the structural anomaly and the transition temperature.

Because the phase transition concerned here is believed to be a first-order phase transition [14], the transition temperature T_t is expressed by the relation

$$T_t = \frac{\Delta H}{\Delta S} \tag{11}$$

where ΔH and ΔS are the enthalpy and entropy changes at the phase transition point, respectively. X-ray diffraction measurement for urea adducts with *n*-alkanes with $n = 16$–44 revealed that volume change at the phase transition point ΔV is exceptionally large compared with that for other *n*-values [14]. Using the Clausius–Clapeyron relation and equation (11), the values of ΔH and ΔS can be evaluated from the value ΔV, T_t and $\mathrm{d}T_t/\mathrm{d}p$ in the following way:

$$\Delta S = \Delta V\left(\frac{\mathrm{d}T_t}{\mathrm{d}p}\right)^{-1} \qquad \Delta H = T_t\,\Delta V\left(\frac{\mathrm{d}T_t}{\mathrm{d}p}\right)^{-1}. \tag{12}$$

Figure 8 shows the *n*-dependence of ΔS and ΔH obtained using equation (12). The values of ΔV, T_t and $\mathrm{d}T_t/\mathrm{d}p$ listed in [14] were used for obtaining both ΔS and ΔH. The values of ΔS and ΔH both show a peak around $n = 20$. Because ΔS and ΔH are directly related to the crystal structure and arrangement of urea adducts with *n*-alkanes, this is part of the experimental evidence that the structural anomaly raises the transition temperature of *n*-eicosane/urea adducts. In order to elucidate the relationship between the structure and

the T_t completely, we should make a detailed energy calculation for both the high- and low-temperature phases and perform a structural analysis for the low-temperature phase.

Acknowledgments

The experimental part of this work was done during the author's stay in Freiburg as an Alexander von Humboldt Research fellow. The author would like to express his cordial thanks to Professor G Strobl for useful discussions and to the Alexander von Humboldt Stiftung for financial support.

References

[1] Smith A E 1952 *Acta Crystallogr.* **5** 224
[2] Chatani Y, Anraku H and Taki Y 1978 *Mol. Cryst. Liq. Cryst.* **48** 219
[3] Cho Y, Kobayashi M and Tadokoro H 1986 *J. Chem. Phys.* **84** 4636, 4643
[4] Wood K A, Snyder R G and Strauss H L 1989 *J. Chem. Phys.* **91** 5255
[5] Kobayashi M, Koizumi H and Cho Y 1990 *J. Chem. Phys.* **93** 4659
[6] Fukao K, Miyaji H and Asai K 1986 *J. Chem. Phys.* **84** 6360
[7] Forst R, Jagodzinski H, Boysen H and Frey F 1987 *Acta Crystallogr.* B **43** 187
[8] Fukao K 1994 *J. Chem. Phys.* **101** 7882, 7893
[9] Guillaume F, Sourisseau C and Dianoux A J 1990 *J. Chem. Phys.* **93** 3536
[10] Guillaume F, Sourisseau C and Dianoux A J 1991 *J. Chim. Phys. (Paris)* **88** 1721
[11] Fukao K 1990 *J. Chem. Phys.* **92** 6867
[12] Harris K D M 1993 *J. Solid State Chem.* **106** 83
[13] Guillaume F, El Baghdadi A and Dianoux A J 1993 *Phys. Scr.* T **49** 691
[14] Fukao K, Horiuchi T, Taki S and Matsushige K 1990 *Mol. Cryst. Liq. Cryst.* B **180** 405
[15] Frey F 1995 *Acta Crystallogr.* B **51** 592
[16] Laves F, Nicolaides N and Peng K C 1965 *Z. Kristallogr.* **121** 258
[17] Tadokoro H 1979 *Structure of Crystalline Polymers* (New York: Wiley)
[18] Parsonage N G and Pemberton R C 1966 *Trans. Faraday Soc.* **63** 311